



Wear Behavior of Vanadium and V-Ti-Ta Alloys under Reciprocating Sliding Conditions

U. Jain , K. Sairam, K. Singh, and R. Tewari

(Submitted February 28, 2019; in revised form April 9, 2019; published online May 14, 2019)

Vanadium and newly developed V-Ti-Ta alloys have been systematically investigated for wear characteristics using ball-on-flat reciprocative sliding experiments. These materials have been tested at different sliding conditions (load and frequency) against hardened steel (AFBMA Grade 10) ball as counter-body. Coefficient of friction, wear volume and specific wear rate were measured and evaluated. Friction coefficient of vanadium and its alloys increases with increase in applied load irrespective of sliding frequencies. Wear rate decreases with increase in alloying content. Among the investigated compositions, V-4Ti-7Ta alloy exhibited superior wear performance having a least wear rate of $3.06 \times 10^{-6} \text{ mm}^3/\text{Nm}$, which is three times lower as compared with unalloyed vanadium when tested at 5 N and 5 Hz conditions. Addition of Ti and Ta strengthens the vanadium matrix by solid solution and contributes to enhanced wear resistance of the material without affecting the friction coefficient values. The major phases identified in the wear track regions were V_2O_5 and $\text{Fe}_{0.11}\text{V}_2\text{O}_{5.15}$. Microstructural investigation reveals the predominant presence of adhesive wear regions at higher loads (15 N).

Keywords coefficient of friction, microstructures, phase analysis, reciprocative sliding, vanadium, wear rate

1. Introduction

Vanadium alloys and steel are the potential candidate materials for fast neutron reactor due to their attractive properties like high temperature strength, low neutron-induced activation characteristics and strong resistance to neutron irradiation (Ref 1-6). These materials sustain high temperatures in liquid sodium environment (working temperatures up to 550 °C) during normal reactor operating condition (Ref 1-6). Vanadium has gained an increased attention of the researchers as it provides flexibility of extending reactor operation temperatures up to 700 °C (Ref 4), where steel suffers poor creep resistance (Ref 5) at that high-temperatures regime. Hence, opting for vanadium as structural material would give an edge of operating future/advanced fast neutron reactors beyond 550 °C, which is the existing molten sodium pool temperature. Among published reports till date (Ref 7-11), V-4Cr-4Ti alloy is reported to exhibit good high temperature stability, strength and low neutron activation criteria. In another study, tantalum (Ref 11, 12) is reported to be an effective solid solution strengthening element compared with other elements (Cr, Mo, Nb, Ta, Ti and W) that satisfies low neutron activation criteria (Ref 10, 13). In order to strengthen the vanadium alloy, Jain et al. (Ref 14) have recently developed a novel vanadium

alloy with titanium and tantalum as solid solution agents satisfying the low neutron activation criteria as well and reported its thermodynamic properties.

In fast neutron reactor, the structural materials such as fuel rod and control rod cladding assemblies are reported to undergo “wear” during its service conditions majorly due to the relative motion of the subassemblies as well as caused by flow-induced vibrations in reactor pool (Ref 15, 16). Thus, it is worth to explore the tribological aspects of vanadium alloys, which are one of the proposed structural materials in fast reactor assemblies. The work of Garcia et al. (Ref 17) is one of the few reports in the literature that probed the modifications in wear properties of V alloys (V-5%Ti alloy) by surface treatment procedures. However, the reported study lacks information on the wear mechanisms that are active in the vanadium and its alloys. In view of this gap, the present study is focused on the wear resistance of unalloyed vanadium and newly developed V-Ti-Ta alloys. For this purpose, reciprocating sliding wear tests under dry sliding conditions and hardened steel ball counter-body on unalloyed vanadium and V-4Ti-(1-7) Ta alloys were carried out. The present study is aimed at investigating the wear characteristics of unalloyed vanadium metal with respect to wear testing parameters and understanding the effect of alloying additions on wear behavior.

2. Experimental Procedure

2.1 Sample Preparation

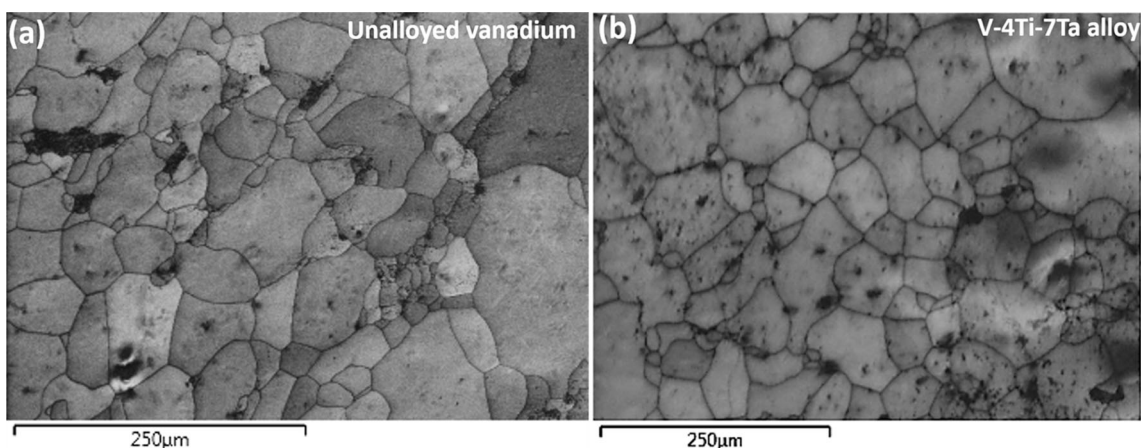
V-4Ti alloys with varying compositions of Ta (1, 3 and 7 wt.%) were prepared in a non-consumable vacuum arc furnace. Chemical composition and calculated neutron absorption cross section of base metal (vanadium) and alloying elements (titanium and tantalum) are given in Table 1. Samples were melted multiple times to ensure better homogeneity in mixing. The developed alloys were tested for their composition by x-ray fluorescence (XRF). Alloys were cold rolled and subsequently

U. Jain, K. Sairam, and R. Tewari, Materials Group, Bhabha Atomic Research Centre, Trombay, Mumbai 400085, India; and Homi Bhabha National Institute, Anushakti Nagar, Mumbai 400094, India; and K. Singh, Materials Group, Bhabha Atomic Research Centre, Trombay, Mumbai 400085, India. Contact e-mails: uttamniff04@gmail.com and uttamj@barc.gov.in.

Table 1 Composition and material properties

Material	Elements, wt.%			Calculated fast neutron absorption cross section (millibarn, mb) (a)	Vickers hardness, MPa
	V	Ti	Ta		
V	99.90 ± 0.05	1.3	150 ± 5
Ti (material used for alloying)	...	99.90 ± 0.10	...	1.2	...
Ta (material used for alloying)	99.80 ± 0.12	50	...
V-4Ti-1Ta	95.20 ± 0.20	3.95 ± 0.05	0.8 ± 0.02	1.4	165 ± 8
V-4Ti-3Ta	93.25 ± 0.18	4.10 ± 0.20	2.6 ± 0.05	1.7	180 ± 7
V-4Ti-7Ta	89.40 ± 0.26	3.90 ± 0.10	6.6 ± 0.12	2.3	215 ± 10

(a) Theoretical neutron cross section of alloys calculated by considering the atomic proportion of the individual alloying elements using nist database (Ref 34)

**Fig. 1** (a, b) SEM micrograph of annealed (a) unalloyed vanadium and (b) V-4Ti-7Ta alloy samples used as base materials for wear testing

annealed at 1200 °C in 10⁻⁵ mbar vacuum. Annealed samples were ground and polished to 1-μm surface finish. These polished samples were taken as base samples for all experiments. The microstructure of starting base material (unalloyed vanadium and V-4Ti-7Ta alloy) obtained using scanning electron microscope (SEM Zeiss EV040) is shown in Fig. 1(a) and (b).

2.2 Wear Experiments

Wear experiments were conducted on unalloyed vanadium and on developed alloys (V-4Ti-(1-7)Ta) in dry unlubricated condition at room temperature with 60% relative humidity, using a ball-on-flat reciprocative sliding wear and friction machine (Plint TE 70SLIM Micro-friction, DUCOM, India). The schematic of the wear testing configuration has been reported elsewhere (Ref 18). Hardened steel ball (AFBMA Grade 10, diameter 10 mm) was used as a counter-body material. Samples were subjected to normal loads of 5, 10 and 15 N with varying sliding frequencies (5-15 Hz) keeping an amplitude of 1 mm for 100-min duration.

2.3 Sample Characterization

Wear debris were collected on an adhesive tape and analyzed for their phase(s) using x-ray diffraction technique (MoK α , XRD). Wear scars were characterized for surface topography, depth and volume using non-contact 3D optical

profilometer (CCIMP3D, Taylor Hobson, UK). Microstructure of wear track regions was also investigated using SEM-EDS. In order to understand the micro-chemistry of wear track regions, electron spot pattern analysis was performed. Unalloyed vanadium and the developed alloys were tested for their mechanical properties (hardness and yield strength) using Vickers's micro-hardness tester (ESEWAY4000TM, Innovatest, Netherland) and miniature tensile testing machine (5kN module, Deben UK). Hardness was measured using the applied load of 0.5 kg for 15 s dwell time (Refer Table 1). Yield strength of the annealed samples was measured using miniature tensile samples having gauge length, width and thickness of 5.1, 1 and 0.3 mm, respectively, with a crosshead speed of 0.04 mm min⁻¹ in room-temperature condition. Coefficient of friction was recorded as a function of sliding distance/time. Wear rate was derived using the measured wear volume, applied normal load and total sliding distance (Eq 1). The data reported in the present study are an average of five wear experiments under each condition.

$$\text{Specific wear rate} \left(\frac{\text{mm}^3}{\text{N} \times \text{m}} \right) = \frac{\text{Wear volume (mm}^3\text{)}}{\text{Load (N)} \times \text{Total sliding distance (m)}} \quad (\text{Eq 1})$$

3. Results and Discussion

3.1 Coefficient of Friction (COF)

COF of unalloyed vanadium and V-4Ti-(1-7)Ta alloys was recorded at different loads (5-15 N) and frequencies (5-15 Hz) conditions for a fixed duration of 100 min. COF of unalloyed vanadium as a function of time is shown in Fig. 2(a), (b) and (c). The mean coefficient of friction obtained as a function of different loads (5, 10 and 15 N) for constant sliding frequencies of 5 Hz and 15 Hz for unalloyed vanadium and its alloys is given in Fig. 3(a), (b) and (c).

It was observed that at 5 Hz and 5 N conditions, the mean COF recorded for unalloyed vanadium sample was 0.39. At 5 Hz, upon increasing the normal load from 5 to 15 N, the COF of vanadium was found to vary from 0.39 to 0.51, respectively. At 15 N normal load, variation in sliding frequency from 5 Hz to 15 Hz resulted in marginal decrease in COF from 0.51 to 0.46 in unalloyed vanadium sample. Similar to unalloyed vanadium, the developed vanadium alloy samples also exhibited identical trend in COF with respect to the applied normal load (Fig. 3a, b, and c). On comparing vanadium and its alloys, it was noticed that the inclusion of alloying elements results in only marginal variation in COF values. It infers that any variation in normal load impacts the mean COF values as compared with changes in the sliding frequency condition and alloying additions. The strong dependence of COF on applied load shall be explained as follows: The higher is the normal load, the higher would be the stress generated which would result in severe fracturing and fragmentation of the investigated material and contribute to increased COF values.

3.2 3D Profilometry

Figure 4(a) and (b) shows the 3D optical profilometric results obtained for an unalloyed sample tested at (a) 5 N and 15 Hz and (b) 15 N and 15 Hz loading conditions, respectively. Surface profiles of worn regions consist of abraded abrasive regions with continuous grooves parallel to the sliding directions. The derived cross-sectional depth profiles show the presence of shallower (42 μm) and deeper (65 μm) grooves, when tested at 5 and 15 N conditions, respectively, for a constant frequency of 15 Hz. The wear volume obtained using optical profilometry for unalloyed vanadium was measured to vary from 2.9×10^{-3} to 2.5×10^{-2} mm^3 corresponding to 5 and 15 N conditions, respectively. The V-Ti-Ta alloys also exhibited similar trend in measured wear volume with respect

to the changes in loading conditions. This profilometric results corroborate the dominance of applied load on the wear behavior of the material. Figure 5(a), (b) and (c) shows wear scar regions of (a) unalloyed vanadium, (b) V-4Ti-3Ta and (c) V-4Ti-7Ta obtained at identical wear testing conditions (5 N and 15 Hz). It was observed that the extent of damage (based on the depth profile) was maximum in unalloyed vanadium sample. However, on increasing the alloying content (Ta), damage intensity decreases, which indicates the enhanced wear performance of the developed alloys compared with unalloyed vanadium. The wear volume measured for V-4Ti-7Ta was 60-70% lower as compared with vanadium metal under similar conditions.

3.3 Wear Rate

Effect of wear testing parameters on wear rate is given in Fig. 6(a), (b) and (c). It was observed that at a constant frequency of 5 Hz, the wear rate of unalloyed vanadium was found to be varying between 9.78×10^{-6} and 2.79×10^{-5} mm^3/Nm , upon increasing the load from 5 to 15 N, respectively. Almost three-time increase in wear rate was observed in unalloyed vanadium with respect to increase in normal load. At 5 N normal load, increase in sliding frequency from 5 to 15 Hz results in only marginal rise in the wear rate of unalloyed vanadium (Fig. 6). Similarly, V-Ti-Ta alloy samples also exhibited identical behavior in wear rates upon increase in normal load irrespective of sliding frequencies tested. It is reported that the other established nonferrous alloy systems like Ti (Ref 19) and Al (Ref 20-23) also exhibited similar trend of increased wear rates with respect to the increase of applied loading condition. This increase in wear rate shall be attributed to the generation of deeper and severe subsurface defects at higher loading conditions. Figure 7(a) and (b) shows the severity of cracks that are formed when sample was tested at 15 N load and the cracking was minimal in case of 5 N condition. Insert in the micrograph shows the two-dimensional depth profile of the wear scar regions tested at 5 N and 15 Hz (Fig. 7a), 15 N and 15 Hz (Fig. 7b) conditions.

Wear rate noticed for V-4Ti-1Ta alloy sample at 5 N and 5 Hz conditions is 8.82×10^{-6} mm^3/Nm which is about 10% lower than the wear rate of unalloyed vanadium sample. At 5 N and 5 Hz, upon increasing the Ta content to 3 wt.%, the wear rate of vanadium alloy was obtained to be 5.01×10^{-6} mm^3/Nm which is about 48% lower in comparison with unalloyed vanadium. V-4Ti-7Ta alloy exhibited a least wear rate of 3.06×10^{-6} mm^3/Nm at 5 N and 5 Hz condition in compar-

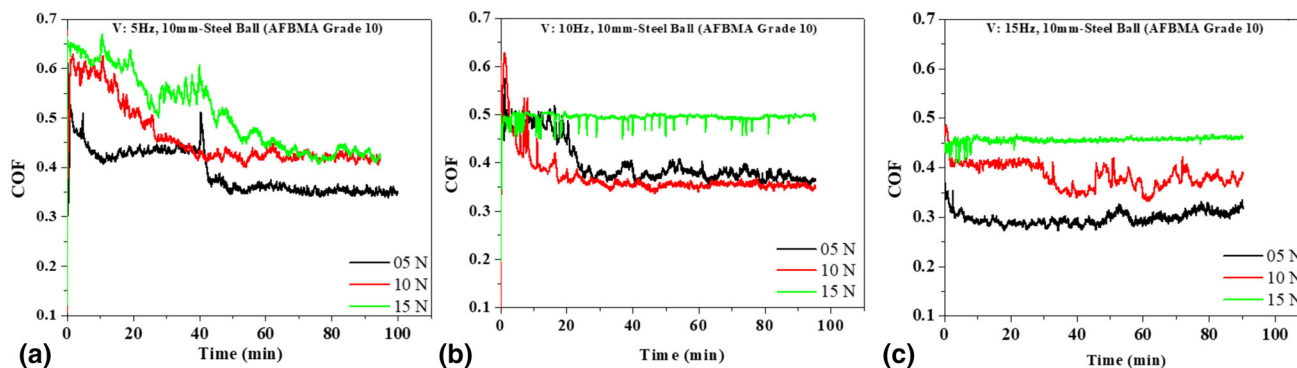


Fig. 2 (a-c) Typical coefficient of friction plots obtained as a function of time for unalloyed vanadium samples tested at different loads (5, 10 and 15 N) for a fixed frequencies of (a) 5 Hz (b) 10 Hz and (c) 15 Hz, respectively

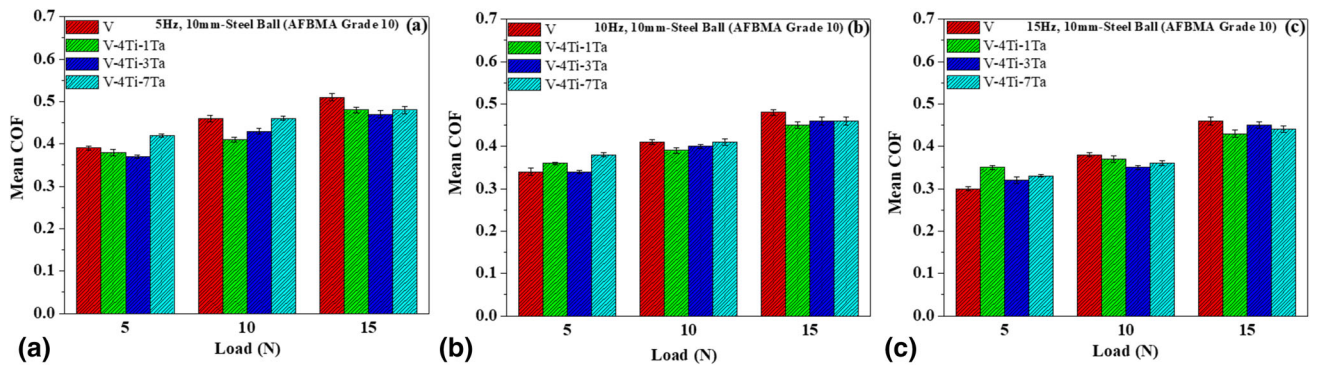


Fig. 3 (a-c) Comparison of mean COF obtained as a function of load at (a) 5 Hz, (b) 10 Hz and (c) 15 Hz frequencies for unalloyed V and V-Ti-Ta alloys

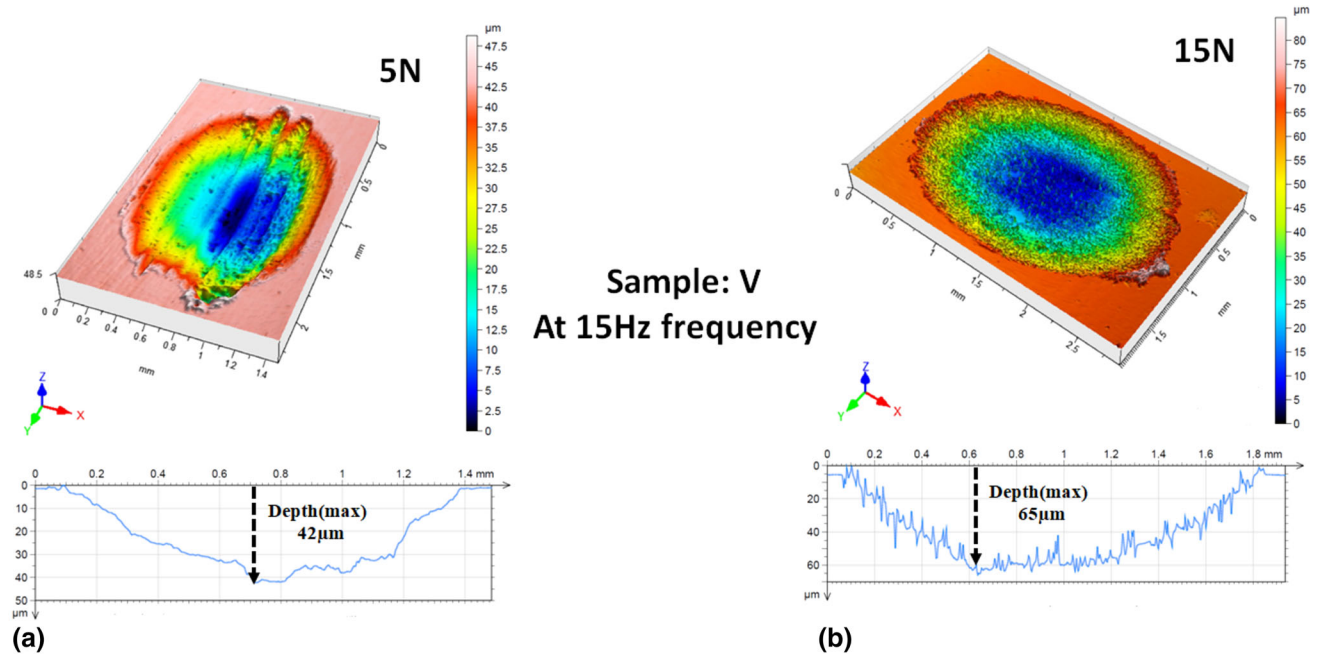


Fig. 4 (a, b) 3D optical profilometry obtained for unalloyed vanadium tested at (a) 5 N and 15 Hz and (b) 15 N and 15 Hz loading conditions showing the presence of shallower (42 μm) and deeper (65 μm) grooves, respectively

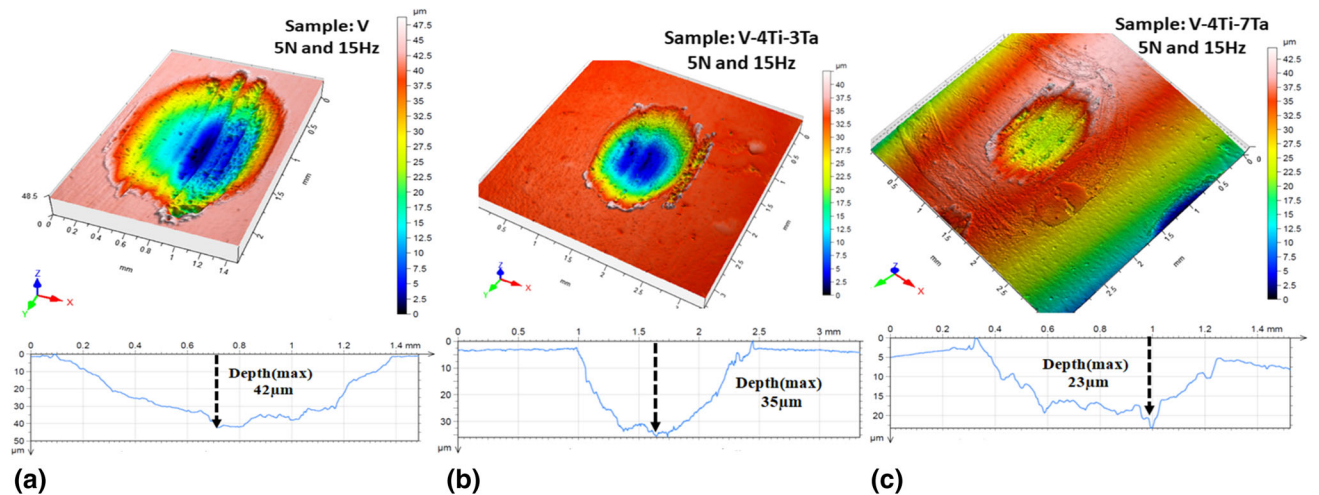


Fig. 5 (a-c) 3D optical profilometric images obtained for 5 N and 15 Hz conditions, showing the extent of damage profile (wear scar regions) with respect to alloying contents [(a) an unalloyed vanadium (b) V-4Ti-3Ta alloy and (c) V-4Ti-7Ta alloy]

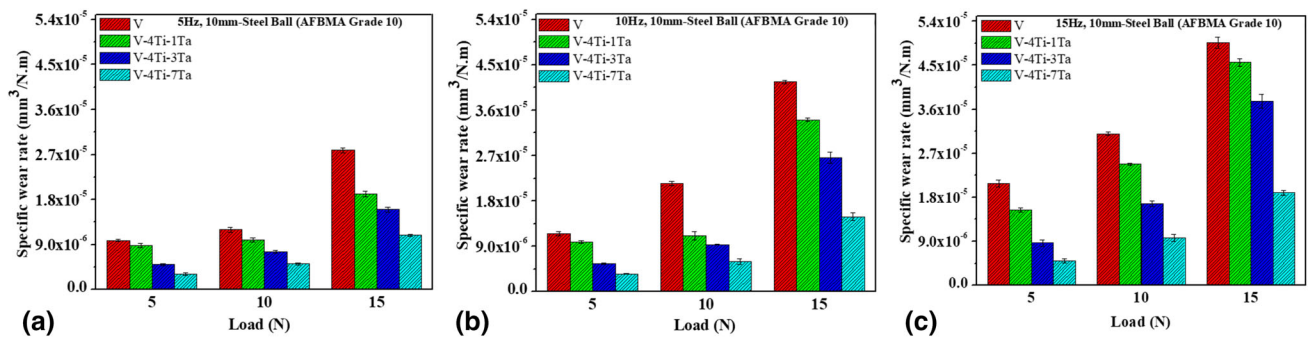


Fig. 6 (a-c) Specific wear rate of unalloyed V and V-Ti-Ta alloys obtained using steel ball as counter-body material. Illustrating improved wear resistance characteristics with respect to alloying additions (Ti and Ta) to V

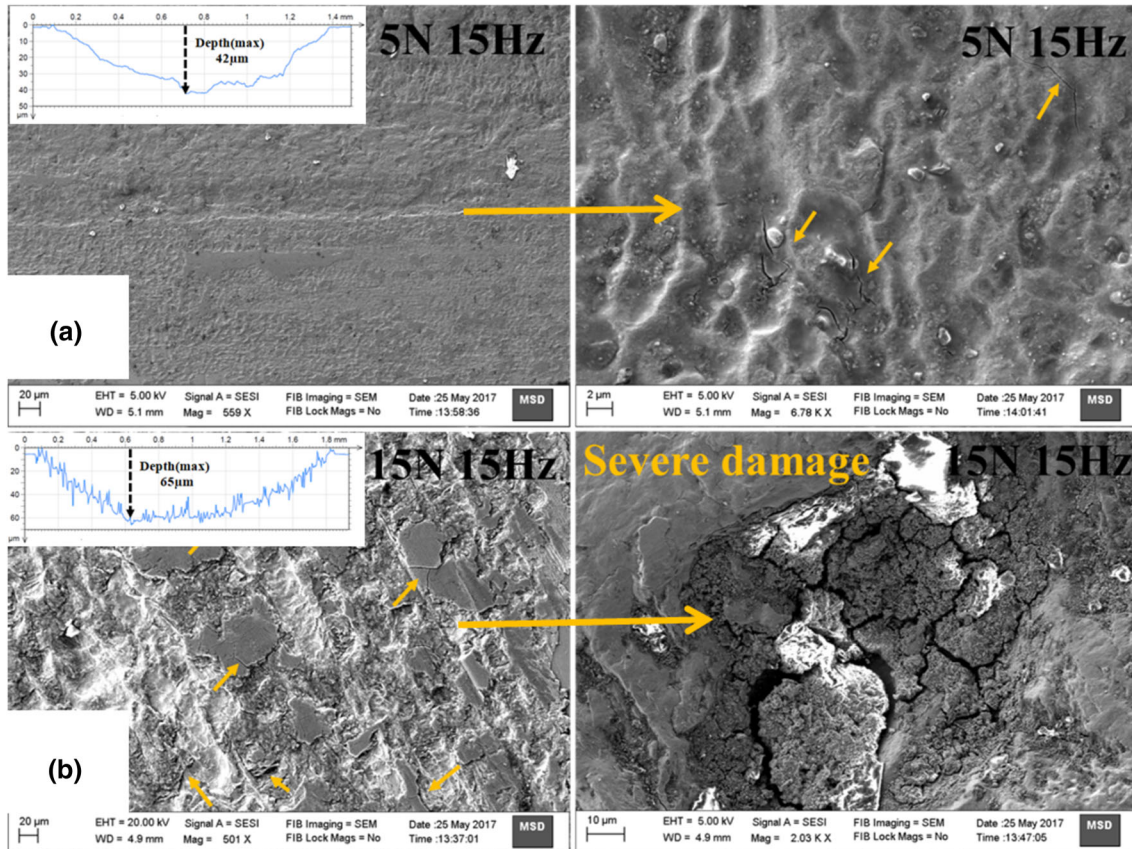


Fig. 7 (a, b) SEM micrograph of unalloyed vanadium sample depicting the severity of the cracks that are formed when the load was increased from (a) 5 N to (b) 15 N; (smaller arrow mark indicates the cracks, and inserts in the micrograph show the corresponding depth profile of the wear scar region obtained using profilometry)

ison with all the investigated samples of this present study. It is evident that wear rate decreases upon alloying Ti and Ta with V and exhibited superior wear performance in comparison with unalloyed vanadium sample. This superior wear performance of V-4Ti-7Ta alloy sample shall be attributed to increased yield strength of the developed material. The yield strengths of unalloyed V and V-4Ti-7Ta alloys are measured to be 200 ± 10 MPa and 600 ± 10 MPa, respectively. Addition of Ti and Ta strengthens the vanadium matrix by solid solution formation and contributes to enhancing the yield strength of the material in the present study. This strengthened matrix offers enhanced resistance to the sliding motion of hardened steel ball when compared with unalloyed vanadium. V-4Ti-7Ta alloy was

measured to exhibit higher hardness (215 MPa) when compared with unalloyed vanadium sample (150 MPa) which also contributes to lowering the wear rate in vanadium alloy sample. Similar observation was reported on the role of yield strength and hardness on improved wear resistance behaviors exhibited by Al and Ti alloys (Ref 24-27).

It is worth to compare the evaluated wear rates of developed vanadium alloys with respect to the established nonferrous alloys such as Al and Ti, which have been commercially exploited for the tribological/engineering applications. On comparison of wear rate data taken under closely matching experimental conditions in the literature (Refer Table 2), it was found that the developed vanadium alloys exhibit two-order

Table 2 Comparison of wear properties of some established nonferrous alloys and the developed alloys of this present study

Material	Counter-body	Test configuration	Sliding speed, m/s	Load, N	Relative humidity	COF	Specific wear rate, mm ³ /Nm	References
Al-2Si	High carbon chromium steel	Pin on disk	0.25	5	60%	...	9×10^{-4}	Torabian et al. (Ref 33)
Al-20Si	High carbon stainless steel	Ball on disk	0.10	5 and 8	...	0.42 and 0.62	9.4×10^{-4} and 6.9×10^{-4}	Liu et al. (Ref 31)
Ti-6Al-4 V	Maraging steel	Pin on flat	0.025	75 and 250	...	0.41 and 0.37	8×10^{-4}	Long et al. (Ref 32)
Ti-6Al-4 V	6-mm-diameter steel ball	Ball on disk	0.10	5	35-45%	0.52	5×10^{-4}	Farokhzadeh et al. (Ref 30)
V-4Ti-1Ta alloy	10-mm-diameter hardened steel ball	Ball on disk	0.01	5	60%	0.38	8.8×10^{-6}	Present study
V-4Ti-3Ta alloy	10-mm-diameter hardened steel ball	Ball on disk	0.01	5	60%	0.37	5×10^{-6}	Present study
V-4Ti-7Ta alloy	10-mm-diameter hardened steel ball	Ball on disk	0.01	5	60%	0.42	3×10^{-6}	Present study

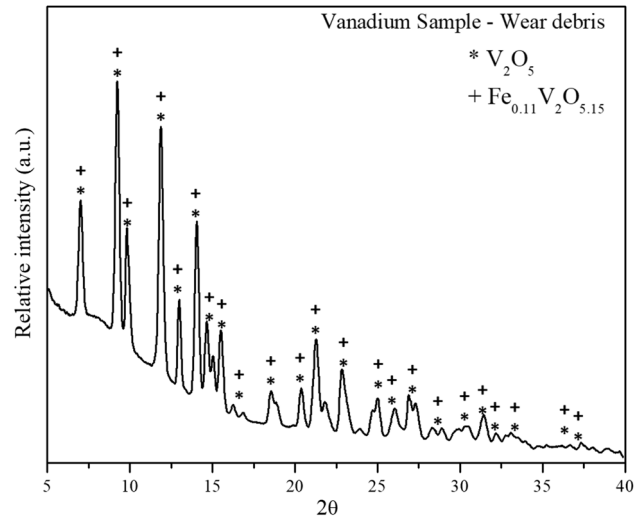


Fig. 8 XRD pattern of wear debris generated from vanadium sample indicates the possible presence of V₂O₅/Fe_{0.11}V₂O_{5.15} crystalline phase

lower wear rate with respect to Al and Ti alloys. The wear rate of Al-Si alloys and Ti-6Al-4 V alloys was reported to be of the order of 10^{-4} mm³/Nm (Ref 27-32), whereas that of developed vanadium alloys is in the range of 10^{-6} mm³/Nm. In view of superior wear characteristics exhibited by the developed vanadium alloys, it warrants to explore the applicability of developed alloys for different tribological applications in addition to nuclear structural material.

3.4 Phase Identification and Microstructural Investigation

Wear debris gathered from unalloyed V and V-Ti-Ta alloys were characterized for their phases and composition. Analyses of XRD patterns obtained from the wear debris of both unalloyed V and V-4Ti-7Ta alloy samples indicated the possible presence of either V₂O₅ or Fe_{0.11}V₂O_{5.15} phases (Fig. 8). As these two mentioned oxide phases maintain close inter-planar spacing, it was difficult to decipher the nature of oxide present in the debris. In order to establish the identity of the oxide phase, detailed EDS analysis of the debris was carried out (Fig. 9). EDS spot pattern analysis indicates the invariable coexistence of regions that are composed of elements like (a) V, Fe and O, (b) V and O and (c) V, Fe, Ti, Ta and O (observed in case of vanadium alloys only). Based on the information obtained from XRD and EDS analyses, the wear scar regions were identified to contain both V₂O₅ and mixed (V-Fe-O) oxide phases. The composition of mixed oxide region was identified to be Fe_{0.11}V₂O_{5.15}. The source of iron in oxide phase could be attributed to come from the hardened steel ball (counter-body) majorly by adhesive wear mechanism. No sign of individual oxides was found in XRD patterns of V-Ti-Ta alloy debris which signifies that elements like Ti and Ta would be associated with vanadium oxide phase in solid solution form.

Electron micrograph of wear scar showed the presence of three distinct regions which were identified as (A) cracked regions, (B) plow regions and (c) solidified regions (Fig. 9a, b, c and d), and the chemical composition obtained from region (A, B and C) is summarized in Table 3. The predominant presence of adhesive wear regions could be noticed in the

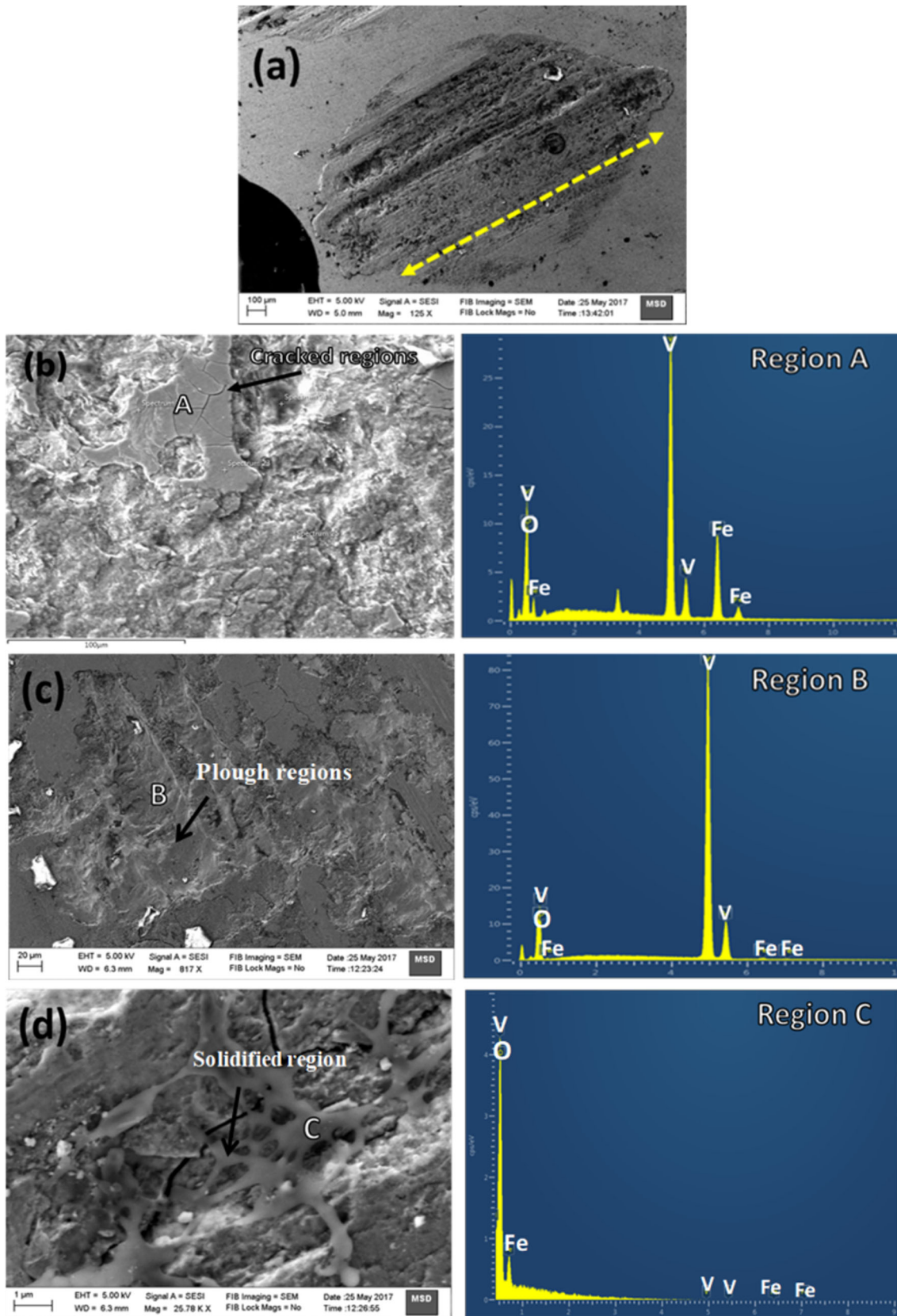


Fig. 9 (a-d) Scanning secondary electron micrograph of worn-out surface vanadium after wear experiment (15 N, 15 Hz) illustrating (a) typical worm scars formed on samples consisting of abraded abrasive regions with continuous grooves parallel to the sliding direction (b) cracked regions, (c) plow regions and (d) solidified regions

Table 3 Chemical characterization of wear scar regions of unalloyed vanadium sample

Name of region	Composition in at.%			
	V	Fe	O	
Region A	Cracked region	30.7	7	62.3
Region B	Smooth deformed region	95.6	0.6	3.8
Region C	Solidified region (solidified V ₂ O ₅)	29.3	0.4	70.3

microstructure of the sample subjected to wear testing at 15 N and 15 Hz conditions (Fig. 9). This kind of morphology was made through squashing and plowing actions of the counter-body material. As sliding continues, the relative motions between base metal (vanadium) and counter-body (hardened steel ball) would generate very high temperatures at the contact points that induce diffusion bonding at its interface. These localized bonds would resist further movement of the counter-body material. Once the load applied exceeds the yield strength of the material, the interface regions undergo plastic deformation and further result in cracking. (Severity of cracking was realized in higher load 15 N condition Fig. 7b.) Further motion of counter-body would result in the oxidation of third body material as well. Evidences of such third body oxides have been found during EDS analysis.

The enhanced wear performance noticed in case of V-Ti-Ta alloy samples shall be correlated with the nature of debris (oxides) formed during wear experiments, as these debris govern the further erosion of the base material. As mentioned in the preceding paragraph, the presence of Ti and Ta elements in solid solution form increases the hardness of vanadium oxides which offers enhanced resistance to the base material erosion, thus contributing to superior wear performance over unalloyed vanadium sample. In general, the reactor subassemblies encounter series of wear events in service conditions and those components are expected to move with greater reliability and with least contact stresses with respect to other critical structural members. The developed alloy (V-4Ti-7Ta) has demonstrated superior wear resistance behavior (68% lower wear rate compared to unalloyed vanadium) without significantly affecting the friction coefficient values, which is of prime importance considering nuclear reactor applications.

4. Conclusion

Vanadium and the newly developed alloys have been tested for wear characteristics using ball-on-flat reciprocative sliding wear experiment.

1. Coefficient of friction of vanadium and its alloys was measured to be in the range of 0.30-0.51 when tested for a normal load of 5 N and 15 N.
2. Increase in normal load increases COF values for both vanadium and its alloys. Application of normal load was found to play a significant role in COF values as compared with sliding frequency. The presence of alloying elements such as Ti and Ta did not found to influence COF as compared with unalloyed vanadium.

3. Almost three-time higher wear rate was noticed in case of vanadium with increase in applied load from 5 N to 15 N. The increase in normal load increases the severity of surface cracking which in turn causes increase in the wear rate of the investigated material.
4. V-4Ti-7Ta alloy exhibited superior wear performance (~ 68% lower wear rate) compared with unalloyed vanadium. The presence of alloying elements such as Ti and Ta increases the yield strength of the material by forming the solid solution and thereby offers increased wear resistance.
5. The presence of elements like Ti, Ta, Fe in solid solution with vanadium oxides (in tribo-layer) enhances the hardness of the oxide which offers enhanced resistance to the base material erosion and contributes to superior wear performance over unalloyed vanadium sample.

Acknowledgments

The authors would like to thank Dr. Madangopal Krishnan, associate director, Materials Group, and Dr. G. K. Dey, Raja Ramanna Fellow, BARC for their consistent support and encouragement related to work. The authors would also like to thank Dr. B. Vishwanadh, MSD, BARC for SEM characterization. The authors are also grateful to Dr. Sanjib Majumdar, MP&CED for extending the wear testing facilities.

References

1. I.A.E. AGENCY, *Structural Materials for Liquid Metal Cooled Fast Reactor Fuel Assemblies-Operational Behaviour* (INTERNATIONAL ATOMIC ENERGY AGENCY, 2012)
2. S.L. Mannan, S.C. Chetal, B. Raj, and S.B. Bhoje, Selection of Materials for Prototype Fast Breeder Reactor, *Trans. Indian Inst. Met.*, 2003, **56**, p 155–178
3. M.D. Mathew, R. Sandhya, and K. Laha, Development of Structural and Steam Generator Materials for Sodium Cooled Fast Reactors, *Energy Procedia*, 2011, **7**, p 250–256
4. G. Edison and G.A. Whitlow, Vanadium Alloys vs Stainless Steel for Sodium-Cooled Fast Reactor Cladding, *Nucl. Appl. Technol.*, 1969, **7**(5), p 443–455
5. S.N. Votinov, V.P. Kolotushkin, S.A. Nikulin, and V.Y. Turilina, Making Vanadium-Based Radiation-Resistant Alloys for Fast-Neutron Reactor Pin Sheaths, *Met. Sci. Heat Treat.*, 2009, **51**(5), p 238
6. D.L. Harrod and R.E. Gold, Mechanical Properties of Vanadium and Vanadium-Base Alloys, *Int. Met. Rev.*, 1980, **25**(1), p 163–222
7. S.N. Votinov, M.I. Solonin, Y.I. Kazennov, V.P. Kondratjev, A.D. Nikulin, V.N. Tebus, E.O. Adamov, S.E. Bougaenko, Y.S. Strebkov, A.V. Sidorenkov, V.B. Ivanov, V.A. Kazakov, V.A. Evtikhin, I.E. Lyublinski, V.M. Trojanov, A.E. Rusanov, V.M. Chernov, and G.A. Birgevoj, Prospects and Problems Using Vanadium Alloys as a Structural Material of the First Wall and Blanket of Fusion Reactors, *J. Nucl. Mater.*, 1996, **233-237**, p 370–375
8. T. Muroga, J.M. Chen, V.M. Chernov, R.J. Kurtz, and M. Le Flem, Present Status of Vanadium Alloys for Fusion Applications, *J. Nucl. Mater.*, 2014, **455**(1-3), p 263–268
9. K. Natesan and M. Uz, Oxidation performance of V-Cr-Ti alloys, *Fusion Eng. Des.*, 2000, **51-52**(Supplement C), p 145–152
10. R.L. Klueh, D.S. Gelles, M. Okada, and N.H. Packan, *Reduced-Activation Materials for Fusion Reactors: An Overview of the Proceedings*, DE89 007199, American Society for Testing and Materials, 1988
11. S.N. Votinov, Vanadium Alloys as Structural Materials for Fusion Reactor Blanket, *Plasma Device Oper.*, 1996, **4**, p 9
12. V.V. Shyrovkov, C.B. Vasylyv, and O.V. Shyrovkov, Ways of Improving the High-Temperature Work Service of Vanadium and Some Alloys used in Reactors, *J. Nucl. Mater.*, 2009, **394**(1), p 114–122

13. M. Victoria, N. Baluc, and P. Spätig, Structural Materials for Fusion Reactors, *Nucl. Fusion*, 2001, **41**(8), p 1047
14. U. Jain, A. Mukherjee, and G.K. Dey, Thermodynamic Properties of Ti in V-Ti-Ta Alloys: Effect of Ta Addition, *J. Alloys Compd.*, 2016, **686**(Supplement C), p 946–950
15. V. Prakash, M. Thirumalai, M. Anandaraj, P.A. Kumar, D. Ramdasu, G.K. Pandey, G. Padmakumar, C. Anandbabu, and P. Kalyanasundaram, Experimental Qualification of Subassembly Design for Prototype Fast Breeder Reactor, *Nucl. Eng. Des.*, 2011, **241**(8), p 3325–3332
16. B. Raj, Materials and Manufacturing Technologies for Sodium Cooled Fast Reactors and Associated Fuel Cycle: Innovations and Maturity, *Energy Procedia*, 2011, **7**, p 186–198
17. J.A. García, R. Rodríguez, R. Sánchez, R. Martínez, M. Varela, D. Cáceres, A. Muñoz, D.I. Vergara, and C. Ballesteros, Tribological Study of Vanadium-Based Alloys Ion Implanted at Low Energy and High Temperature, *Vacuum*, 2002, **67**(3), p 543–550
18. T.S.R.C. Murthy, P.K. Limaye, J.K. Sonber, K. Sairam, A. Nagaraj, C. Subramanian, N.L. Soni, R.J. Patel, and R.C. Hubli, Friction and Wear Properties of Hot Pressed (Ti, Cr)B₂ + MoSi₂ Composite in Sliding Against WC ball, *Int. J. Refract. Met. Hard Mater.*, 2014, **43**, p 276–283
19. S.R. Chauhan and K. Dass, Dry Sliding Wear Behaviour of Titanium (Grade 5) Alloy by Using Response Surface Methodology, *Adv. Tribol.*, 2013, **2013**, p 9
20. R.A. Al-Samaraid, K.A. Haftirman, and Y. Al-Douri, Effect of Load and Sliding Speed on Wear and Friction of Aluminum-Silicon Casting Alloy, *Int. J. Sci. Res. Publ.*, 2012, **2**, p 1–4
21. D. Odabas, Effects of Load and Speed on Wear Rate of Abrasive Wear for 2014 Al Alloy, *IOP Conf. Ser. Mater. Sci. Eng.*, 2018, **295**, p 012008
22. K. Singh, S. Singh, and A. Shrivastava, Comparison of Wear and Friction Behavior of Aluminum Matrix Alloy (Al 7075) and Silicon Carbide based Aluminum Metal Matrix Composite under Dry Condition at Different Sliding Distance, *Mater. Today Proc.*, 2016, **4**(8), p 8960–8970
23. M. Chowdhury, M.K. Khalil, D.M. Nuruzzaman, and M. Rahaman, The effect of sliding speed and normal load on friction and wear property of aluminum, *Int. J. Mech. Mechatron. Eng.*, 2011, **11**, p 53–57
24. D.K. Dwivedi, Wear Behaviour of Cast Hypereutectic Aluminium Silicon Alloys, *Mater. Des.*, 2006, **27**(7), p 610–616
25. S.A. Kori and T.M. Chandrashekharaiiah, Studies on the Dry Sliding Wear Behaviour of Hypoeutectic and Eutectic Al-Si Alloys, *Wear*, 2007, **263**(1), p 745–755
26. R. Dasgupta and S.K. Bose, Effect of Copper on the Tribological Properties of Al-Si Base Alloys, *J. Mater. Sci. Lett.*, 1995, **14**(23), p 1661–1663
27. G.D. Revankar, R. Shetty, S.S. Rao, and V.N. Gaitonde, Wear Resistance Enhancement of Titanium Alloy (Ti-6Al-4 V) by Ball Burnishing Process, *J. Mater. Res. Technol.*, 2017, **6**(1), p 13–32
28. J. Qu, P.J. Blau, T.R. Watkins, O.B. Cavin, and N.S. Kulkarni, Friction and Wear of Titanium Alloys Sliding Against Metal, Polymer, and Ceramic Counterfaces, *Wear*, 2005, **258**(9), p 1348–1356
29. M. Elmadagli, T. Perry, and A.T. Alpas, A Parametric Study of the Relationship Between Microstructure and Wear Resistance of Al-Si Alloys, *Wear*, 2007, **262**(1), p 79–92
30. K. Farokhzadeh and A. Edrisy, Transition Between Mild and Severe Wear in Titanium Alloys, *Tribol. Int.*, 2016, **94**, p 98–111
31. G. Liu, G. Li, A. Cai, and Z. Chen, The Influence of Strontium Addition on Wear Properties of Al-20wt% Si Alloys Under Dry Reciprocating Sliding Condition, *Mater. Des.*, 2011, **32**(1), p 121–126
32. M. Long and H.J. Rack, Friction and Surface Behavior of Selected Titanium Alloys During Reciprocating-Sliding Motion, *Wear*, 2001, **249**(1), p 157–167
33. H. Torabian, J.P. Pathak, and S.N. Tiwari, Wear Characteristics of Al-Si alloys, *Wear*, 1994, **172**, p 49–58
34. <https://www-nds.iaea.org/ngatlas/>

Publisher's Note Springer Nature remains neutral with regard to jurisdictional claims in published maps and institutional affiliations.